Jordi Artigas*
DLR, German Aerospace Center
Institute of Robotics
and Mechatronics
Oberpfaffenhofen, Germany

Jee-Hwan Ryu
School of Mechanical Engineering
Korea University of Technology
and Education
Cheoan-city, 330-708
Republic of Korea

Carsten Preusche
DLR, German Aerospace Center
Institute of Robotics
and Mechatronics
Oberpfaffenhofen, Germany

Time Domain Passivity Control for Position-Position Teleoperation Architectures

Abstract

This article presents a method for passivating the communication channel of a symmetric position-position teleoperation architecture on the time domain. The time domain passivity control approach has recently gained appeal in the context of time-delayed teleoperation because passivity is not established as a design constraint, which often forces conservative rules, but rather as a property which the system must preserve during operation. Since passivity is a network property, the first design rule within this framework is to represent consistent and comprehensible circuit (i.e., network) representations of the mechanical teleoperation system. In particular, the energetic behavior of these networks is interesting because it allows straightforward conclusions about system stability. By means of so-called passivity observers (PO) and passivity controllers (PC) (Hannaford & Ryu, 2001, Time domain passivity control of haptic interfaces, *Proceedings of IEEE ICRA '01*, pp. 1863–1869), the energetic response of a delayed communication channel is captured and modulated over time so that the network in question never becomes nonpassive. The case analyzed in this paper tackles a communication channel that conveys position data back and forth. This type of channel does not offer intuitive network representation since only flows are actually being transmitted. Although energy clearly travels from one side to the other, port power identification, as defined by the correlated pair flow and effort, is not evident. This work first investigates how this kind of channels can be represented by means of circuit networks even with the lack of physical effort being transmitted through the channel, and identifies which networks are susceptible to become nonpassive due to the channel characteristics (i.e., time delay, discretization or package loss). Once achieved, a distributed control structure is presented based on a PC series that keeps the system at the verge of passivity (and therefore stability) independent from the channel properties. The results obtained by the simulation and by experiment sustain the presented approach.

1 Introduction

Telepresence is the feeling of existing in a location other than where the individual actually is, and the capacity of interacting in it. Feelings of being present somewhere else can be artificially induced in individuals by using a set of technologies that capture sensory data from the distant reality, such as

Presence, *Vol. 19, No. 5, October 2010*, 000–000

*Correspondence to jordi.artigas@dlr.de.

AQ1

visual, audio, or haptic information, and reproduce it locally by means of a human-machine interface (HMI). Interaction between individual and distant environment takes place by conveying the individual's actions and reactions, such as spoken commands or manipulation actions, to the distant location. A telerobotic system reproduces the individual's commands. In particular, the haptic channel is appealing because it allows kinesthesia and tactile sense to be remotely reproduced, yielding two fundamental perceptions for environment manipulation. Telepresence thus extends human sensorial and manipulative capabilities to far/unreachable locations. Transparency describes the discrepancy between remote and local presence. Ideal transparency means that the user is not able to distinguish remote presence from local presence.

Bilateral control is the discipline that investigates the closed-loop circuit created between the human operator and the remote environment. Special control methods are applied in order to stabilize a closed loop system that often includes time delay, package loss, unavoidable nonlinearities, and subsystems that cannot be completely modeled, such as the human operator and the remote environment.

The pursuit of stability often compromises transparency once the system constraints are established. This trade-off is a common denominator in every single approach dealing with bilateral control (Lawrence, 1993; Yokokohji & Yoshikawa, 1994). In this sense, one of the most accounted issues in haptic telemanipulation scenarios is the time delay that affects the communication channel. This often leads to the design of conservative control laws in order to achieve unconditional system stability, which in turn often results in system transparency losses.

One of the most remarkable approaches in dealing with time-delayed telepresence is using passivity criteria. Passivity is a sufficient condition for stability and provides the nice feature that system passivity is granted by passivity of all its subsystems. Moreover, passivity of a system can be analyzed without an exact knowledge of its contents. It is therefore a useful tool that can be used as a design rule in those systems that incorporate communication elements, since, as it has been shown (Anderson & Spong, 1989), delay is a source of activity. A good example is the scattering transformation (Anderson & Spong) and its wave variables formulation (Niemeyer, 1996), which has become the classical approach in delayed teleoperation.

Most approaches that deal with delayed teleoperation end up using conservative techniques to the detriment of transparency and usability of the teleoperation system. In order to ensure passivity of the system, bilateral control often introduces elements that dissipate more energy than is strictly needed to compensate for the energy introduced by delayed communications. Wave variable-based methods, for instance, do present a nonlossy characteristic after applying wave transformation; however, damping elements are then needed to minimize wave reflections and to achieve impedance matching (Niemeyer, 1996) between master and slave.

The time domain passivity control approach (TDPC; Ryu, Hannaford, Preusche, & Hirzinger, 2003; Hannaford & Ryu, 2001) presents two main advantages that have garnered attention within the haptics and telerobotics field. The first advantage is the fact that the design is performed considering the ideal case, that is, assuming no time delay in the communication channel and perfect data transmission. The second advantage is that only the observed active energy is dissipated. This allows designs aimed at transparency rather than at passivity. Previous work (Artigas, Preusche, & Hirzinger, 2007; Ryu & Preusche, 2007; Artigas, Preusche, Hirzinger, Borghesan, & Melchiorri, 2008, 2009) have shown feasibility and provide good results. However, they mainly focus on position-force (P-F) architectures, or do not specifically consider the channel as the network to passivate but rather the bilateral control (Ryu & Preusche).

A drawback of the passivity framework is that input and output of the system have to be power conjugated, that is, each input is related to an output and their product must be power. Hence, if only the mechanical domain is considered, inputs and outputs must be generalized velocities and torques (Hannaford, Ryu, & Kim, 2004; Secchi, Stramigioli, & Fantuzzi, 2007). This presents a difficulty when representing a position-position (P-P) system, since a mapping to flow and effort representations is no longer evident. Recently, the passivity of the P-P systems was analyzed (Lee & Spong, 2006), where proportional derivative control and robust control techniques were used. To the best knowledge of the authors, passivity of a communication channel exchanging position in both directions using TDPC has not yet been analyzed. Since passivity can be seen as a network property, the first rule for designing within the time domain framework is to represent consistent and comprehensible circuit representation of the mechanical teleoperation system to be designed. Once the circuit model is described, networks can be identified and analyzed.

This paper begins with a review and a mathematical formulation of the time domain passivity control approach for delayed teleoperation in Section 2. In particular, passivity of time delay power networks (TDPN) is studied in Section 2.2, including how it can be controlled. The energetic behavior of this type of network is vital because it directly allows a conclusion to be made about system stability. As will be seen, by means of so-called passivity observers (PO) and passivity controllers (PC), this behavior is captured and shaped so that the network in question never becomes active. Section 3 tackles the P-P communication channel through investigation of its circuit representation and identification of networks susceptible to become nonpassive due to channel characteristics. Moreover, a distributed control structure based on a PC series is presented that guarantees passivity independently from channel characteristics. Section 4 shows the performance of the system in a simulation environment and Section 5 in an experimental setup. Finally, in Section 6, discussion and results are presented.

2 The Time Delay Power Network (TDPN)

A communication channel interchanging position (or, equivalently, velocity) and force presents the interesting characteristic that it can be modeled by means of a simple network where flow and effort travel in opposite directions. Each port is entirely defined by an undelayed signal (e.g., flow at the left side) and its conjugate delayed signal (effort). Each conjugate pair define a power at each port (Figure 1) which, if integrated over time, results in port energy. This type of channel will from now on be referred to as a time delay power network (TDPN). TDPNs are characterized as: Figure 1

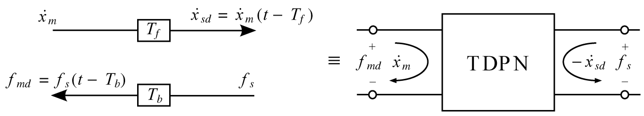

Figure 1. *Two port network representation of a position—force communication channel.*

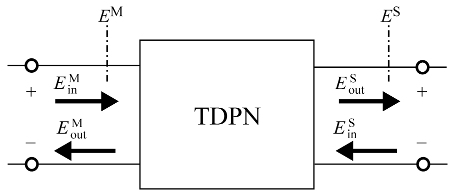

Figure 2. *In and out energies of the time delay power network (TDPN).*

- Two port network communication elements containing an unknown time delay separating both ports.
- Accepting two possible causalities. Velocity traveling forward with force traveling backward (as is the current study case); and the opposite, force traveling forward with velocity traveling backward.
- A fundamental communication element on most teleoperation systems.
- An essential element for the passivity rationale in the time domain (see Figure 2). Figure 2

Once the method on how to establish the passivity rule on a TDPN is clear, the same principle can be applied to other more complex communication structures, where the mapping to effort and flow may not be obvious. For instance, it will be seen how the position-position (P-P) communication channel can be reduced to a pair of TDPNs, allowing clear effort-flow representation and power ports where passivity considerations can be straightforwardly extracted.

2.1 Passivity of the Time Delay Power Network

Using the sign convention defined in Figure 1, the energy of a TDPN can be expressed as:

$$E^{\text{ch}}(t) = E^{\text{M}}(t) + E^{\text{S}}(t) \quad \forall t \geq 0. \tag{1}$$

Where each energy value at left and right ports of the communication channel, $E^{\text{M}}(t)$ and $E^{\text{S}}(t)$ are

$$\begin{aligned} E^{\text{M}}(t) &= \int_0^t P^{\text{M}}(\tau)\,d\tau = \int_0^t f_{\text{md}}(\tau)\dot{x}_{\text{m}}(\tau)\,d\tau, \\ &\qquad \forall t \geq 0, \\ E^{\text{S}}(t) &= \int_0^t P^{\text{S}}(\tau)\,d\tau = \int_0^t -f_{\text{s}}(t)\dot{x}_{\text{sd}}(t)\,d\tau, \\ &\qquad \forall t \geq 0, \end{aligned} \tag{2}$$

and where P^{M} and P^{S} are the master and slave port powers. The TDPN will be passive as long as

$$E^{\text{ch}}(t) \geq 0, \quad \forall t \geq 0. \tag{3}$$

The methods presented in this paper are based on time domain passivity control, whose only requirement is that network energy flow must be observable in time. Unfortunately, E^{ch} cannot be observed in realistic scenarios since both port energies, E^{M} and E^{S}, cannot be simultaneously available. In the following, it is shown how this energy can be observed even in the presence of time delay.

AXIOM 1: *The energy flow observed at a port of a network, E, can be split into positive and negative components, each of which indicates the direction of propagation.*

We split the positive and negative port power as:

$$\begin{aligned} P_+(t) &= P(t) \quad \forall f(t), v(t) \quad s.t. \\ &\qquad f(t)v(t) > 0, \quad \forall t \geq 0, \\ P_-(t) &= -P(t) \quad \forall f(t), v(t) \quad s.t. \\ &\qquad f(t)v(t) < 0, \quad \forall t \geq 0. \end{aligned} \tag{4}$$

The positive and negative contributions of the energy flow are then

$$E_+(t) = \int_0^t P_+(t)\,d\tau, \quad \forall t \geq 0,$$

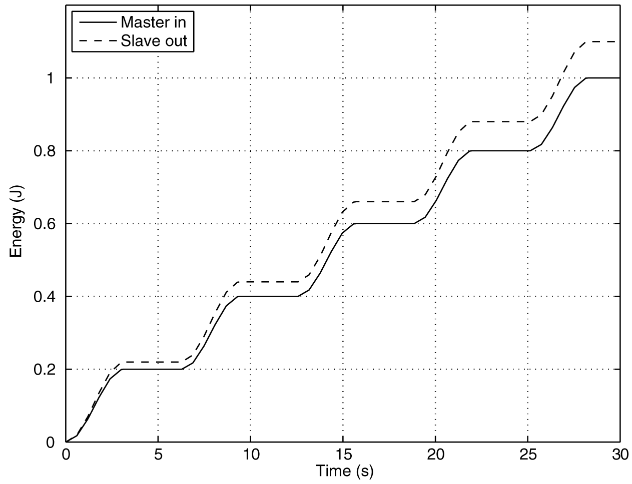

Figure 3. *Master sent energy vs. slave received energy. Typical delayed channel active behavior.*

$$E_-(t) = \int_0^t P_-(t)\,d\tau, \quad \forall t \geq 0, \tag{5}$$

which are both being monotonic and positive defined.

DEFINITION 1: *Input and output components of left and right port energies are related to positive and negative power as:*

$$\begin{aligned} E^{\text{M}}_{\text{in}}(t) &= E^{\text{M}}_+(t), \quad E^{\text{M}}_{\text{out}}(t) = E^{\text{M}}(t), \\ E^{\text{S}}_{\text{in}}(t) &= E^{\text{S}}_+(t), \quad E^{\text{S}}_{\text{out}}(t) = E^{\text{S}}(t), \quad \forall t \geq 0. \end{aligned} \tag{6}$$

Using Definition 1 and Equation 3, energy flow of a TDPN can be expressed as:

$$\begin{aligned} E^{\text{ch}}(t) = E^{\text{M}}(t) + E^{\text{S}}(t) &= E^{\text{M}}_{\text{in}}(t) - E^{\text{M}}_{\text{out}}(t) \\ &+ E^{\text{S}}_{\text{in}}(t) - E^{\text{S}}_{\text{out}}(t). \end{aligned} \tag{7}$$

where the subscript *in* refers to the energy that is injected into the channel from either side and *out* is the energy coming out from the channel.

Equation 6 gives monotonic functions that describe the energy exchange between both sides of the TDPN. Ideally *in* values should match *out* values at the other side. Figure 3 shows typical responses of *in* and *out* values of a delayed communication channel. **Figure 3**

Using *in* and *out* components, passivity of the channel can therefore also be checked using the decoupled energy flow expressions:

$$
\begin{aligned}
E^{\mathrm{ch}}(t) &= E^{\mathrm{M2S}}(t) + E^{\mathrm{S2M}}(t) \geq 0, \quad \forall t \geq 0, \\
E^{\mathrm{M2S}}(t) &= E^{\mathrm{M}}_{\mathrm{in}}(t) - E^{\mathrm{S}}_{\mathrm{out}}(t), \quad \forall t \geq 0, \\
E^{\mathrm{S2M}}(t) &= E^{\mathrm{S}}_{\mathrm{in}}(t) - E^{\mathrm{M}}_{\mathrm{out}}(t), \quad \forall t \geq 0.
\end{aligned} \tag{8}
$$

where E^{M2S} and E^{S2M} are the flows from left to right and from right to left, respectively. Equation 3 holds as long as both of the following constraints are satisfied:

$$
\begin{aligned}
E^{\mathrm{M2S}}(t) \geq 0, \quad \forall t \geq 0, \\
E^{\mathrm{S2M}}(t) \geq 0, \quad \forall t \geq 0.
\end{aligned} \tag{9}
$$

As mentioned above, E^{ch} is an energy that is not observable in a real system. Instead, the following monitorable *observed energies* can be used that represent the flow from left to right monitored at the slave port and the flow from right to left monitored at the master port:

$$
\begin{aligned}
E^{\mathrm{M2S}}_{\mathrm{obs}}(t) &= E^{\mathrm{M}}_{\mathrm{in}}(t - T_{\mathrm{f}}) - E^{\mathrm{S}}_{\mathrm{out}}(t), \quad \forall t \geq 0 \\
&\qquad \text{(observed at the right)} \\
E^{\mathrm{S2M}}_{\mathrm{obs}}(t) &= E^{\mathrm{S}}_{\mathrm{in}}(t - T_{\mathrm{b}}) - E^{\mathrm{M}}_{\mathrm{out}}(t), \quad \forall t \geq 0 \\
&\qquad \text{(observed at the left)}
\end{aligned} \tag{10}
$$

where T_{f} and T_{b} are forward and backward time delays. Equation 10 will give valid flows as long as Equation 9 holds.

THEOREM 1: *If both observed energy flows of a TDPN are $E^{\mathrm{M2S}}_{\mathrm{obs}}(t) \geq 0$ and $E^{\mathrm{S2M}}_{\mathrm{obs}}(t) \geq 0$ then the system is passive (Ryu et al., 2007).*

PROOF: Checking passivity can be done by proving Equation 3. Since both $E^{\mathrm{S}}_{\mathrm{out}}$ and $E^{\mathrm{M}}_{\mathrm{out}}$ are monotonic by definition (from Equation 6), the following holds:

$$
\begin{aligned}
E^{\mathrm{S}}_{\mathrm{out}}(t - T_{\mathrm{b}}) \leq E^{\mathrm{S}}_{\mathrm{out}}(t), \quad \forall t \geq 0, \\
E^{\mathrm{M}}_{\mathrm{out}}(t - T_{\mathrm{f}}) \leq E^{\mathrm{M}}_{\mathrm{out}}(t). \quad \forall t \geq 0,
\end{aligned} \tag{11}
$$

The observed decoupled energy expressions, $E^{\mathrm{M2S}}_{\mathrm{obs}}$ and $E^{\mathrm{S2M}}_{\mathrm{obs}}$ from Equation 10, are thus lower bounded by
Fn 1 the decoupled real[1] expressions, E^{M2S} and E^{S2M} from Equation 8. That is:

1. The term real is used here to distinguish between actual energy and observed energy.

$$
\begin{aligned}
E^{\mathrm{M2S}}_{\mathrm{obs}}(t) \leq E^{\mathrm{M2S}}(t), \quad \forall t \geq 0, \\
E^{\mathrm{S2M}}_{\mathrm{obs}}(t) \leq E^{\mathrm{S2M}}(t). \quad \forall t \geq 0.
\end{aligned} \tag{12}
$$

Therefore if constraints $E^{\mathrm{M2S}}_{\mathrm{obs}}(t) \geq 0$ and $E^{\mathrm{S2M}}_{\mathrm{obs}}(t) \geq 0$ are satisfied, so is Equation 9, and thus so is Equation 3.

It is clear from Equation 12 that there exists an error between real and observed energies. Conditions in Equation 12 add in fact some conservatism in the sense that some more energy must be dissipated than is strictly needed. This error can be seen as a passive energy leak and is actually the current energy accumulated in the communication and can obviously not be measured a priori due to the nature of the delayed system. An exact computation would be possible by using a precise model of the time delay. In real scenarios, however, time delay is hard, if not impossible, to model (e.g., radio links, UDP internet connections, etc.). Passivity is a powerful tool precisely in such contexts, this is, where things are hard to model and predict.

2.2 Passivity Observer and Passivity Controller

Once the flows to check for passivity of the communication channel are identified, the passivity observer (PO) and passivity controller (PC) can be defined. Briefly, the TDPC has two main elements: the PO monitors the energy flow of a network in the time domain; and the PC acts as a variable damper to dissipate active energy observed by the PO, that is, it is introduced by the network (see Ryn et al., 2003; Hannaford & Ryu, 2001, for complete PO/PC formulation). From Equation 10 it is clear that passivity of the channel can be checked by monitoring the two flows. Each flow is determined by a source, the energy flow coming from the opposite side, and a sink, the current local port value and the delayed value of the flow coming from the opposite side. This introduces the requirement of a distributed structure involving two observers placed on either side of the communication network. The PO is nothing else than an algorithmic extrapolation of Equation 10 plus the correction introduced by the PC to satisfy passivity. The two POs are thus defined as:

$$\begin{aligned} W_S(n+1) &= E^M_{in}(n-T_f) - E^S_{out}(n) + E^S_{PC}(n), \\ W_M(n+1) &= E^S_{in}(n-T_b) - E^M_{out}(n) + E^M_{PC}(n), \end{aligned} \tag{13}$$

where M and S accompanying the observed energy, W, stand for master and slave observers, corresponding to the right and left side of the communication, respectively. Both E^M_{PC} and E^S_{PC} (later defined in Equation 15) are master and slave dissipated energies by both forward passivity controller (FPC) and backward passivity controller (BPC), respectively. Their specific expressions are dependent on the causality of the local PC.

As in Hannaford and Ryu (2001), the PC comes in the form of a variable damping that adapts as a function of the observed flow. If the observer indicates active behavior, the damping coefficient, α, must be such that it dissipates the active energy. In the admittance configuration (velocity is modified to produce the dissipation) the controller at the right side is described as:

$$\dot{x}_{sd}(n) = \hat{\dot{x}}_{sd}(n) - \frac{1}{\alpha(n)} f_s(n), \tag{14}$$

where $\hat{\dot{x}}_{sd}(n)$ is the untouched velocity signal coming from the master. The α coefficient can be obtained as:

$$\frac{1}{\alpha(n)} = \begin{cases} 0 & \text{if} \quad W_S > 0 \\ \dfrac{-W_S}{f^2(n)} & \text{else, if} \quad |f| > 0 \end{cases}$$

and the dissipated energy is:

$$E^S_{PC}(n) = \Delta T \sum_{k=1}^{k=n-1} f^2(k) \frac{1}{\alpha(n)}. \tag{15}$$

Applying Equation 14 keeps $W_S \geq 0$, which in turn keeps $E^{M2S}_{obs} \geq 0$ and therefore $E^{M2S} \geq 0$ (Equation 9). In a similar way, the PC controller for the impedance case (i.e., velocity is conserved while force is modified to produce dissipation) can be defined. The network created by the system Master PO/PC + TDPN + Slave
Figure 4 PO/PC, as seen in Figure 4, is thus a passive one:

$$E^M_{PC}(n) + E^{ch}(n) + E^S_{PC}(n) \geq 0 \tag{16}$$

The position-force (P-F) architecture is the direct application of the TDPN. As shown above, an

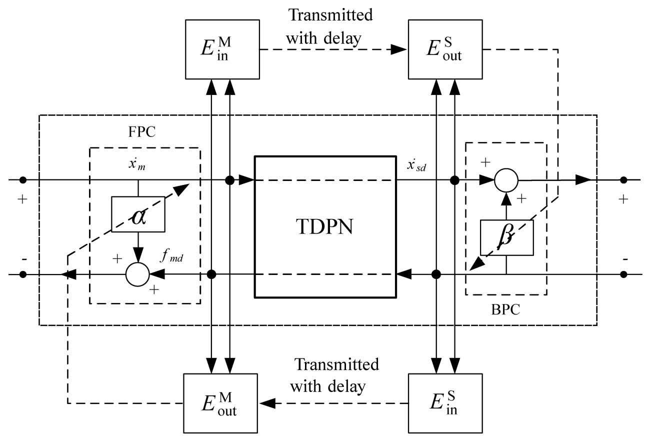

Figure 4. *Passivated TDPN using master and slave PO/PC.*

impedance/admittance PO/PC pair inserted right next to each port of the TDPN will passivate the channel. As observed in Artigas et al. (2008), the P-F scheme presents two drawbacks: it only allows impedance PCs on the left side, which usually produce higher noise levels due to fast activation and deactivation of control forces; and the dissipation on velocity on the right side without position feedback, which may result in position drift. This motivates the use of a Position-Position (P-P) architecture.

3 Position-Position Architecture

As mentioned above, a communication channel that transfers position data in both directions does not present the clear network representation that the TDPN does, since flow and effort do not have direct correspondence with the data exchanged in the channel. The first step to analyze the P-P architecture is to identify the communication channel in a comprehensive network representation to allow examination of the system in terms of energy flow. As will be seen, the P-P communication channel can in fact be represented by means of TDPNs. By extracting and expanding the analogous electrical scheme (using the electrical-mechanical analogy) the system unveils a network arrangement that allows segmentation of active energy due to delays. In particular, two *delayed* dependent current sources are,

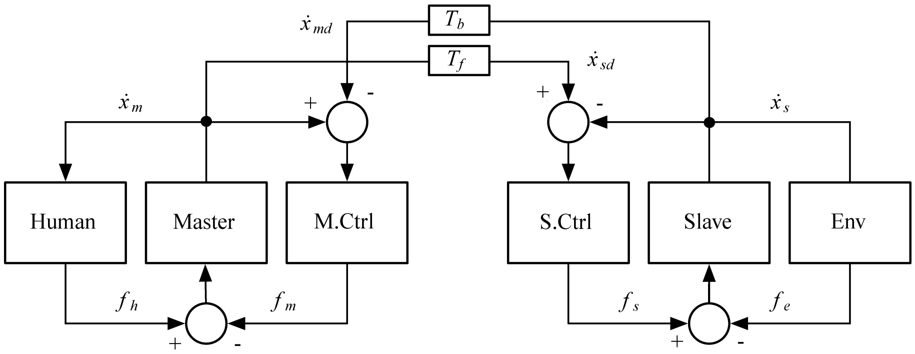

Figure 5. *Bloc diagram of P-P architecture.*

as will be seen, the cause of TDPN masking. Once the P-P TDPN networks are identified, a pair of PO/PC will be placed at each TDPN side in order to guarantee their passivity. The analysis begins with an overview of the architecture used.

3.1 System Description

Figure 5 The scheme is as shown in Figure 5. Both master and slave controllers are PI (PD equivalent when referring to position) linked with local and distant velocities. The desired command for the slave PI is the current master velocity delayed. The controller can thus immediately obey with a force response on the slave device. At the master side, the desired command is the current master velocity, which in turn is the operator's motion intention, and the distant slave is the process to be controlled. While this architecture usually presents higher degrees of resistance to the user as the delay increases compared to the P-F scheme, the P-F, as mentioned above, suffers from higher degrees of noise and position drift.

The equations describing the system are:

$$\begin{aligned} f_{\mathrm{m}}(t) &= K_{\mathrm{dm}}(\dot{x}_{\mathrm{m}}(t) - \dot{x}_{\mathrm{s}}(t - T_{\mathrm{b}})) \\ &\quad + K_{\mathrm{pm}}(x_{\mathrm{m}}(t) - x_{\mathrm{s}}(t - T_{\mathrm{b}})) \\ f_{\mathrm{s}}(t) &= K_{\mathrm{ds}}(\dot{x}_{\mathrm{m}}(t - T_{\mathrm{f}}) - \dot{x}_{\mathrm{s}}(t)) \\ &\quad + K_{\mathrm{sp}}(x_{\mathrm{m}}(t - T_{\mathrm{f}}) - x_{\mathrm{s}}(t)) \end{aligned} \tag{17}$$

where f_{m}, x_{m} and f_{s}, x_{s} are master and slave computed force and position, respectively, and T_{b} and T_{f} are forward and backward delays; and K_{dm}, K_{pm}, K_{ds}, and K_{ps} are derivative and proportional gains for master and slave, respectively. The master dynamics are:

$$\begin{aligned} (f_{\mathrm{h}}(s) - f_{\mathrm{m}}(s))\frac{1}{m_{\mathrm{m}}s^2 + b_{\mathrm{m}}s} &= x_{\mathrm{m}}(s), \\ f_{\mathrm{h}}(s) &= \dot{x}_{\mathrm{m}}(s)Z_{\mathrm{h}}(s). \end{aligned} \tag{18}$$

where f_{h} is the human force; m_{m} and b_{m} are master mass and damping coefficients, and Z_{h} is the human impedance.[2] Equations at the slave side can be obtained in a similar way. Fn 2

3.2 TDPN Identification Through Network Representation

The system can be represented using electrical components as shown in Figure 6. By the duality between the mechanical and electrical systems, it is understood that mechanical signals or elements exhibit identical mathematical behavior to that of the electrical case, although clearly they are physically different.[3] In the present context, the circuit representation also provides the means to describe the P-P architecture as a chain of connected networks. In particular, the two port network signalized in Figure 6, known as N_Z from now on, contains the communication channel.[4] However, Figure 6 Fn 3 Fn 4

2. These equations are purely for explanatory purposes. Note the methods exposed in this paper are independent from master and slave dynamics.
3. The main analogous quantities are: force $\longleftrightarrow$ voltage; and velocity $\longleftrightarrow$ current.
4. Note the same sign convention as in Equation 2 has been used.

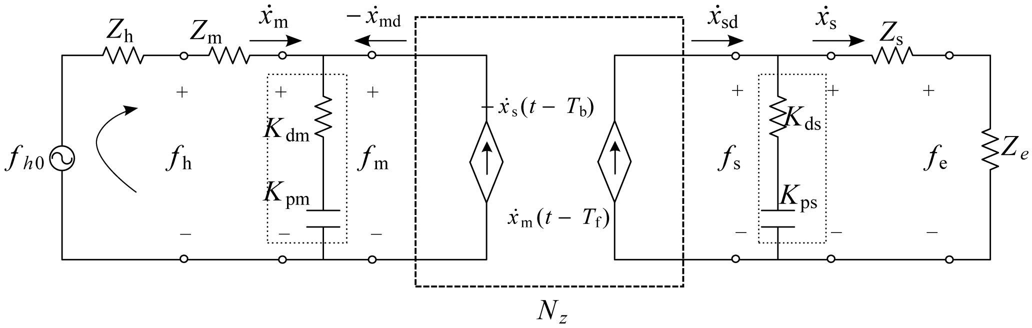

Figure 6. *Circuit representation of a P-P architecture.*

a wrong assumption would be to consider N_Z as only a model of the channel. As can be seen, the network encompasses two dependent current sources. The left source is dependent on previous values of slave velocity while the one on the right is dependent on previous values of master velocity:

$$\begin{aligned} \dot{x}_{md}(t) &= \dot{x}_s(t - T_b), \quad \forall t \geq 0, \\ \dot{x}_{sd}(t) &= \dot{x}_m(t - T_f), \quad \forall t \geq 0. \end{aligned} \tag{19}$$

The energy of N_Z can be expressed as:

$$\begin{aligned} E_{Nz}(t) = E_{Nz1} + E_{Nz2} = \int_0^t &(f_m(\tau)\dot{x}_{md}(\tau) \\ &- f_s(\tau)\dot{x}_{sd}(\tau))\, d\tau, \quad \forall t \geq 0. \end{aligned} \tag{20}$$

This representation indeed describes the behavior of the system; however, as will be shown, it is not accurate enough to isolate the channel from the rest of the circuit, since the two delayed dependent current sources do not solely represent the communication channel. In particular, it would be handy to find a network that resembles the TDPN (see Figure 2) where the passivity analysis is clear.

AXIOM 2: *The network N_z, containing two delayed dependent current sources (Figure 6), can be represented by the combination of two undelayed dependent current sources and two TDPNs carrying the energy of each*
Figure 7 *undelayed dependent current source, see Figure 7.*

This augmented representation is obtained by bringing the delayed dependent current sources to its undelayed location through the networks N_A and N_B, where both are of TDPN type. It is clear now that N_Z not only carries the energy due to the delay, but also the energy due to the current sources C_a and C_b. This can be seen by expanding Equation 20 as follows:

$$\begin{aligned} E_{Nz}(t) &= \int_0^t (f_m(\tau)\dot{x}_s(\tau - T_b) \\ &\qquad - f_s(\tau)\dot{x}_m(t - T_f))\, d\tau \\ &= E_{Na}(t) + E_{Ca}(t) + E_{Nb}(t) + E_{Cb}(t), \end{aligned} \tag{21}$$

where E_{Na} and E_{Nb} are the energy flows of N_A and N_B; and E_{Ca} and E_{Cb} the energy flows of the current sources attached to N_A and N_B, respectively. E_{Na} and E_{Nb} are therefore energy flows traveling through TDPN types of networks, that is, with clear flow and effort pairs defined at each port. Their discrete expressions can be written as:

$$\begin{aligned} E_{Na}(n) &= \Delta T \sum_{k=0}^{k=n} -\dot{x}_s(k) f_m(k - T_b) \\ &\qquad + \dot{x}_s(k - T_b) f_m(k), \\ E_{Nb}(n) &= \Delta T \sum_{k=0}^{k=n} \dot{x}_m(k) f_s(k - T_f) \\ &\qquad - \dot{x}_m(k - T_f) f_s(k) \end{aligned} \tag{22}$$

where ΔT is the sampling time. Furthermore, the energy flow in the discrete domain of the current sources C_a and C_b are as follows:

$$\begin{aligned} E_{Ca}(n) &= \Delta T \sum_{k=0}^{k=n} f_m(k - T_b)\dot{x}_s(k), \\ E_{Cb}(n) &= \Delta T \sum_{k=0}^{k=n} -f_s(k - T_f)\dot{x}_m(k). \end{aligned} \tag{23}$$

This new representation allows for the segmentation of the energy flow introduced by the TDPNs, that is, the

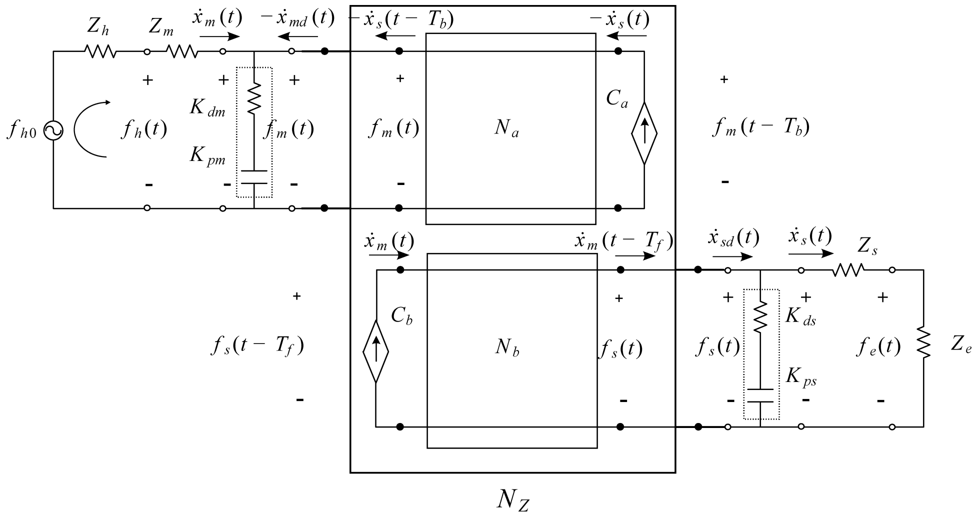

Figure 7. *The network N_z can be segregated within two dependent current sources, C_a and C_b, and two TDPNs, N_a and N_b.*

flow produced by the delay, from the rest of the system. Clearly, the only admissible energy sources in N_Z are both C_a and C_b. The pursuit of channel passivity therefore goes through observation and passivation of $E_{Na}(n)$ and $E_{Nb}(n)$. Note that in the ideal situation, $T_f = 0$ and $T_b = 0$, and both $E_{Na}(n)$ and $E_{Nb}(n)$ become null.

THEOREM 2: *A P-P system with delay in the communication channel will be passive if both of its TDPNs, N_a and N_b, are kept passive (assuming human, master, slave, and PD controllers are passive)*

PROOF: Using Definition 1 and Equation 8, both port energies of N_z in Equation 20, E_{Z1} and E_{Z2}, can be written as:

$$E_{Z1}(t) = E_{Na}(t) + E_{Ca}(t) = E_{Na}^{\mathrm{L2R}}(t) + E_{Na}^{\mathrm{R2L}}(t) + E_{\mathrm{in}}^{\mathrm{Ca}}(t) + E_{\mathrm{out}}^{\mathrm{Ca}}(t),$$
$$E_{Z2}(t) = E_{Nb}(t) + E_{Cb}(t) = E_{Nb}^{\mathrm{L2R}}(t) + E_{Nb}^{\mathrm{R2L}}(t) + E_{\mathrm{in}}^{\mathrm{Cb}}(t) + E_{\mathrm{out}}^{\mathrm{Cb}}(t),$$

where $E_{\mathrm{in}}^{\mathrm{Ca/b}}$ and $E_{\mathrm{out}}^{\mathrm{Ca/b}}$ are the in and out components of $E_{Ca/b}$. And $E_{\mathrm{Na/b}}^{\mathrm{L2R}}$ and $E_{\mathrm{Na/b}}^{\mathrm{R2L}}$ are the left-to-right and right-to-left components, that is, decoupled as in Equation 8.

LEMMA 1: *In a system composed of the cascade of a TDPN and an ideal current source, effective energy can only travel from the current source to the TDPN. E_{Na}^{L2R} and E_{Nb}^{R2L} are canceled out by $E_{\mathrm{in}}^{\mathrm{Ca}}$ and $E_{\mathrm{in}}^{\mathrm{Cb}}$, respectively.*

PROOF: The current through an ideal current source is independent of the voltage across it. The internal resistance of an ideal current source is infinite.[5] (setting the source with zero current as identical to an ideal open circuit). The voltage at the port of an ideal current source is thus completely determined by the circuit it is connected to. When connected to an external load, for instance, the voltage across the source approaches infinity as the load resistance approaches infinity (an open circuit). The power of the an ideal current source is independent from the internal resistance (due to its infinite value) and is proportional to the voltage (positive or negative) across the source. Thus, an ideal current source can supply and absorb unlimited power forever, and so it represents an unlimited source of energy. Therefore, the energy flows toward C_a and C_b, $E_{\mathrm{Na}}^{\mathrm{L2R}}$ and E_{Nb}^{R2L}, are canceled out by $E_{\mathrm{in}}^{\mathrm{Ca}}$ and $E_{\mathrm{in}}^{\mathrm{Cb}}$, respectively.

Fn 5

E_{Z1} and E_{Z2} can thus be rewritten as:

$$E_{Z1}(t) = E_{Na}^{\mathrm{R2L}}(t) + E_{\mathrm{out}}^{\mathrm{Ca}}(t),$$
$$E_{Z2}(t) = E_{Nb}^{\mathrm{L2R}}(t) + E_{\mathrm{out}}^{\mathrm{Cb}}(t). \tag{24}$$

5. The internal resistance of a current source is modeled in parallel with the source.

Therefore, making N_a and N_b passive requires only the following two conditions:

$$E_{Na}^{R2L}(t) \geq 0, \quad E_{Nb}^{L2R}(t) \geq 0. \tag{25}$$

E_{out}^{Cb} represents the amount of energy from the master transferred to the slave. It is assumed that in the system created by C_b, the slave and environment is passive. Note this is not a severe constraint, since it implies that the energy produced on one side is dissipated on the other side without taking the delay into account. The same reasoning is applied for E_{out}^{Ca} (where the human is assumed to be a passive system as well). This is,

$$\begin{aligned} E_{out}^{Cb}(t) + E_{Slave}(t) + E_{ENV}(t) \geq 0, \\ E_{out}^{Ca}(t) + E_{Master}(t) + E_{H}(t) \geq 0. \end{aligned} \tag{26}$$

Using Equations 24 and 26 and the conditions in Equation 25, system passivity is proved as:

$$\begin{aligned} E_H(t) + E_{Master}(t) + E_{Z1}(t) + E_{Z2}(t) + E_{Slave}(t) \\ + E_{ENV}(t) \geq 0, \ \forall t \ \geq 0. \end{aligned} \tag{27}$$

3.3 Passivity Observer and Passivity Controller for P-P Architectures

As seen in Equation 27, the energy flows to be observed and controlled are given in Equation 25, since E_{Na}^{R2L} and E_{Nb}^{L2R} are the energies introduced by the delay. In order to determine both PO and PC expressions, the same procedure seen in Section 2.2 to observe the energy flow for the TDPN is here applied for both N_A and N_B networks. Thus, E_{Na} and E_{Na} can be split into master and slave in and out energies:

$$\begin{aligned} E_{Na}(t) &= E_{in}^{Ma}(t) - E_{out}^{Sa}(t) + E_{in}^{Sa}(t) - E_{out}^{Ma}(t) \\ &= E_{Na}^{L2R}(t) + E_{Na}^{R2L}(t). \end{aligned} \tag{28}$$

$$\begin{aligned} E_{Nb}(t) &= E_{in}^{Mb}(t) - E_{out}^{Sb}(t) + E_{in}^{Sb}(t) - E_{out}^{Mb}(t) \\ &= E_{Nb}^{L2R}(t) + E_{Nb}^{R2L}(t), \end{aligned} \tag{29}$$

where E_{in}^{Ma} for instance, stands for the in energy to network N_a at the master side (the left port of N_a); E_{out}^{Sb} stands for the out energy of N_b at the slave side. Using Equations 4 and 5, expressions of $E_{in/out}^{Ma}$, $E_{in/out}^{Sa}$, $E_{in/out}^{Mb}$, and $E_{in/out}^{Sb}$ can easily be derived.

As shown in Equation 24, only energies flowing from the ideal current source to the circuit are effective. Therefore, a PC is placed at the left port of N_a controlling E_{Na}^{R2L}; and a PC is placed at the right port of N_b controlling the energy flow E_{Nb}^{L2R}.

The POs are defined as:

$$\begin{aligned} W_s(n) &= E_{in}^{Mb}(n - T_f) - E_{out}^{Sb}(n) + E_{PC}^{S}(n) \\ E_{in}^{Mb}(n) &= f(f_s(n - T_f), \dot{x}_m(n)) \\ E_{out}^{Sb}(n) &= g(f_s(n), \dot{x}_m(n - T_f)) \\ &\quad \text{for } N_B \text{ (from master to slave).} \end{aligned}$$

$$\begin{aligned} W_m(n) &= E_{in}^{Sa}(n - T_b) - E_{out}^{Ma}(n) + E_{PC}^{M}(n) \\ E_{in}^{Sa}(n) &= f(f_m(n - T_b), \dot{x}_s(n)) \\ E_{out}^{Ma}(n) &= g(f_m(n), \dot{x}_s(n - T_b)) \\ &\quad \text{for } N_A \text{ (from slave to master).} \end{aligned}$$

where W_s and W_m are the observed energies at slave and master side respectively, and $E_{PC}^{S/M}$ are the dissipated energy by the PC, that is, the update of $E_{out}^{Sb/Ma}$. Note that, f and g are functions that compute in and out energies as in Equations 4 and 5. The PCs are then implemented as in Equation 14.

Passivity is proved using the same reasoning as in Section 2.2, with the difference that only the flow from the current source to the network is considered. Taking this into account and Equations 11 and 12, passivity on the time domain is guaranteed since:

$$\begin{aligned} E_{in}^{Sa}(n) - E_{out}^{Ma}(n) + E_{PC}^{M}(n) \geq 0, \\ E_{in}^{Mb}(n) - E_{out}^{Sb}(n) + E_{PC}^{S}(n) \geq 0, \end{aligned} \tag{30}$$

The system integrating the controllers can be seen in Figure 8. Figure 8

4 Simulations

Master and slave robots are simulated (Matlab Simulink) as mass-damper systems with mass $M_r = 1$ kg and viscous friction of $B_r = 0.3$ Ns/m. The HO is simulated in a closed-loop system that generates the force

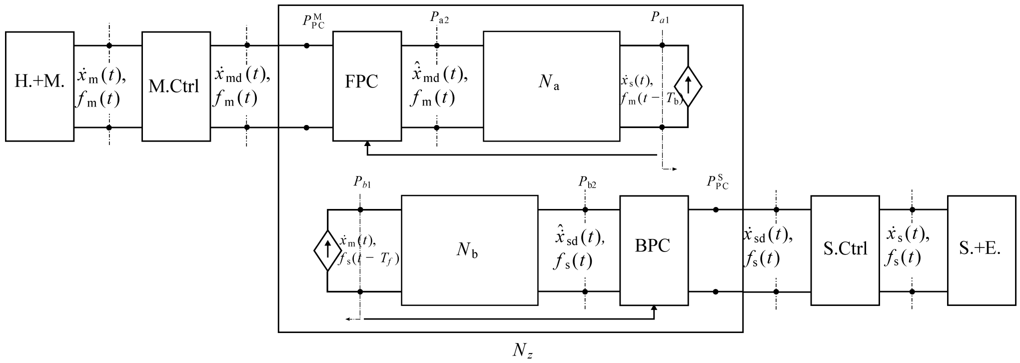

Figure 8. *The system is augmented with FPC and BPC which keep the communication channel passive.*

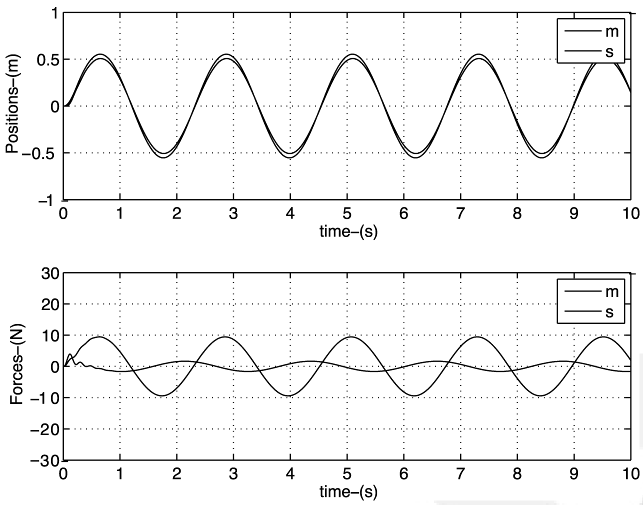

Figure 9. *Master and slave positions and forces for the undelayed case.*

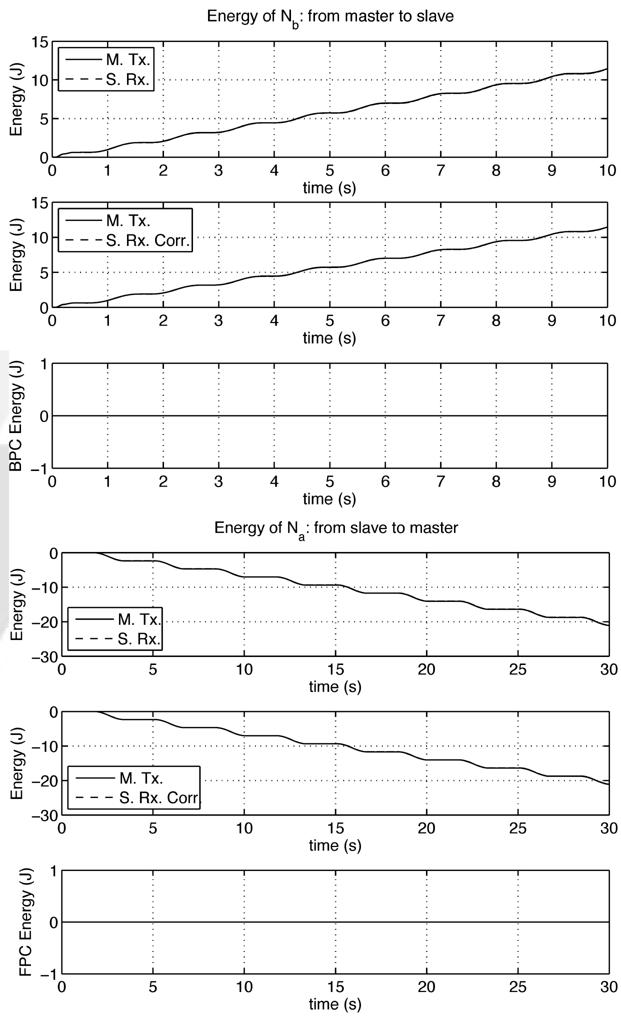

Figure 10. *Observed energies in N_z for the undelayed case.*

to the master robot in order to follow a sinusoidal reference position with frequency of 0.25 Hz and amplitude of 0.25 m. The control part of the system (Master PD, Slave PD, FPC, and BPC) runs at a sampling rate of $T = 1$ ms.

The gain parameters of both PD controllers were tuned using the Nyquist stability criterion such that the system is able to absorb a worst case round trip delay of 20 ms. Performance is first analyzed in the undelayed system; Figure 9 shows master and slave position and forces. The subplot in Figure 10(a) shows the sent

Figure 9
Figure 10

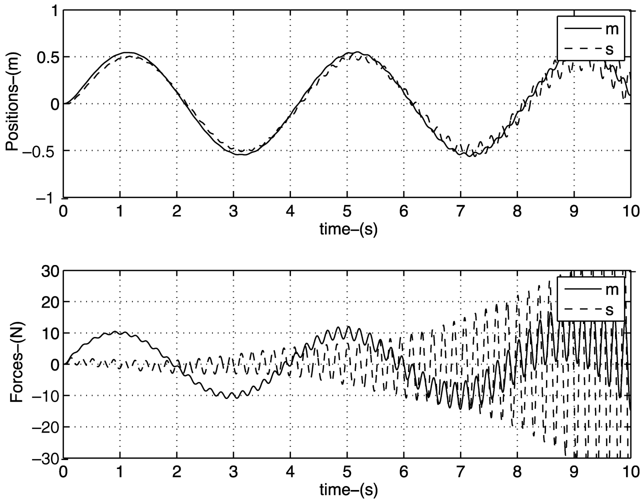

Figure 11. *Master and slave positions and forces with 30 ms delay. Unstable behavior.*

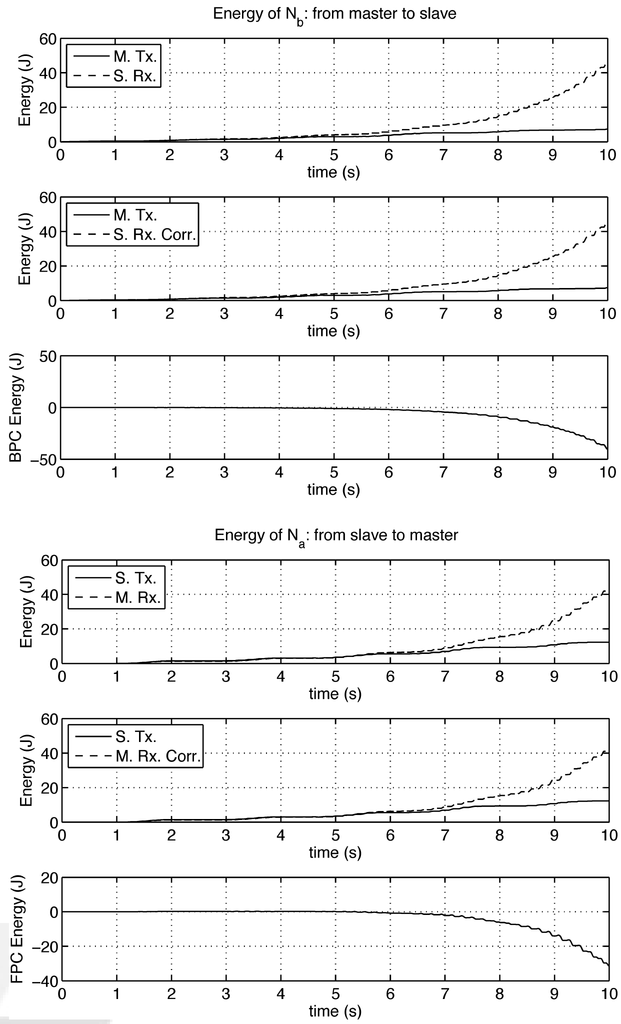

Figure 12. *Observed energies in N_z.*

and received energies of N_b that are obviously identical, since no delay is present in the channel. Figure 10(b) show the same plots for N_a. In order to see energetic responses as the delay increases, a simulation was performed, inserting a delay slightly higher than the maximum allowed by the stability region for which
Figure 11 the system was designed. Figure 11 shows the result-
Figure 12 ing unstable behavior. Figure 12(a,b) show the activity of the channel, that is, more energy is received than sent and the observed energies by the POs are negative. Thus, both networks N_a and N_b are active and the cause of the unstable behavior. The same system has been simulated with both FPC and BPC and has shown stability for any arbitrary communication delay. The results are shown in the next section in an experimental setup.

5 Experiments

The setup uses the same control scheme employed for the simulations in Section 4. Master and slave systems are both DLR, leight weight robots (LWR III), with 7 DOF and masses of around 20 kg. For testing purposes, only the fourth joint of both robots was coupled. Both robots are real time driven by VxWorks at a sampling rate of 1 kHz. The PD controllers were tuned such that the system can allow delays up to $T_{rt} = 5$ ms (when both passivity controllers are deactivated). The following experiments are shown: (a) $T_{rt} = 100$ ms
in a free environment, as shown in Figures 13 and 14; **Figure 13**
(b) $T_{rt} = 100$ ms in hard wall contact, as shown in **Figure 14**
Figures 15 and 16; (c) $T_{rt} = 240$ ms in hard wall con- **Figure 15**
tact, as shown in Figures 17 and 18; and (d) $T_{rt} =$ **Figure 16**
500 ms in hard wall contact, as shown in Figures 19 **Figure 17**
and 20. **Figure 18**

Note the different energy responses before and after **Figure 19**
the PCs in Figures 14, 16, 18, and 20. The first plots **Figure 20**
(the left plots) show N_a and/or N_b active behavior; the second plots (the right plots) show passive networks, that is, N_a plus FPC; and N_b plus BPC. Since

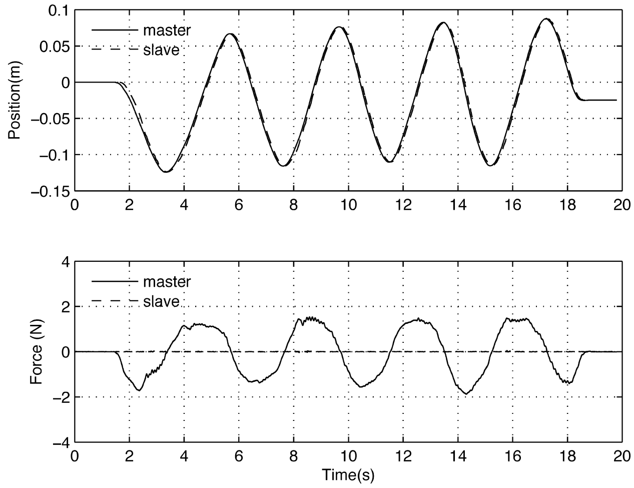

Figure 13. *Experimental data. 100 ms round trip delay. Free environment.*

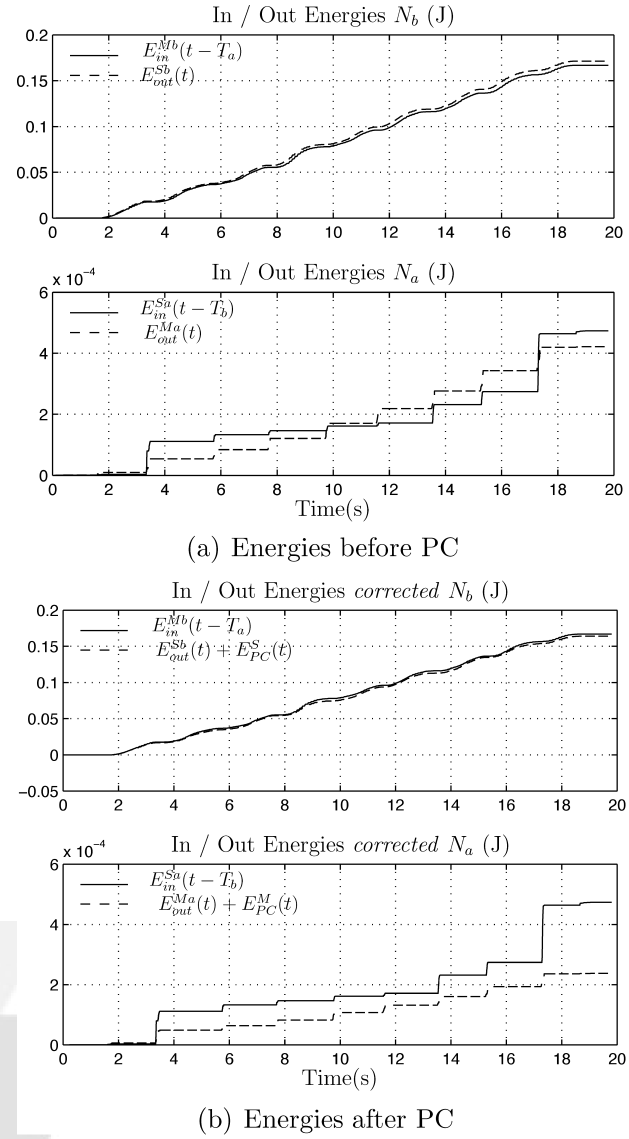

Figure 14. *Experimental data. 100 ms round trip delay. Free environment.*

the user actively moves the master, the energy flows mainly from left to right. The channel mostly generates energy toward the slave side as well, that is, N_b has a more active tendency and therefore the BPC is triggered frequently.

5.1 Discussion

An offset between desired and current position may appear which in turn outputs in a constant force. This is an issue of the P-P architecture since both FPC and BPC modify desired velocities to produce the dissipation. The desired position is obtained by integrating the modified velocity signal and further the PD controller produces the necessary torque to satisfy the desired command. Since observed energy E_{obs}^{ch} (Equation 10) is used instead of real channel energy E^{ch} (Equation 1), more energy is dissipated than strictly needed, and thus an offset can appear. In a P-F architecture, this may result in position drift. In the P-P, since the master and slave are linked with current positions, it may result in a force accumulation which, if big enough, it may be felt by the user. While this is not critical in normal conditions, it can become an issue if delay is large and variable. With the setup presented here, force accumulation could be felt at delays starting from 0.5 s. Solutions to that will be presented in future work.

6 Conclusions

In this work the authors further exploit the potentiality of the bilateral time passivity control approach in order to guarantee stability for P-P teleoperation architectures. It has been shown how a communication channel that exchanges desired positions in both directions can be represented by means of two port networks. A main contribution of this work is the rationale on how

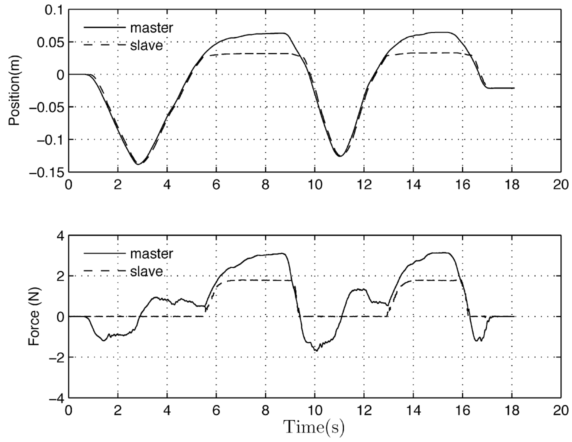

Figure 15. *Experimental data. 100 ms round trip delay. Contact.*

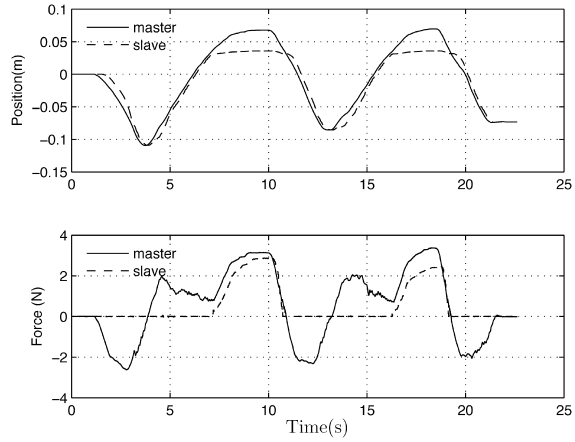

Figure 17. *Experimental data. 240 ms round trip delay. Contact.*

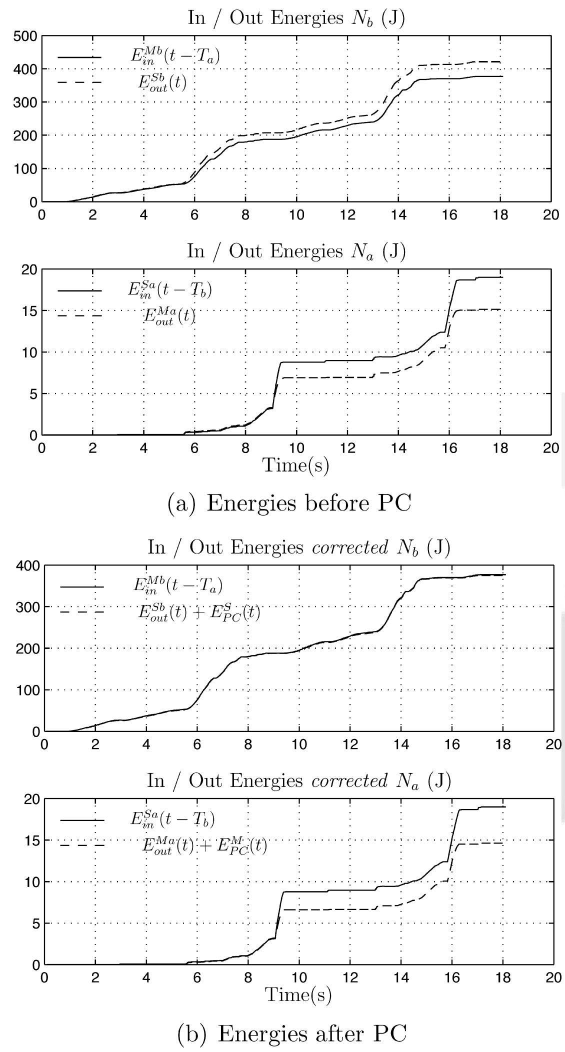

Figure 16. *Experimental data. 100 ms round trip delay. Contact.*

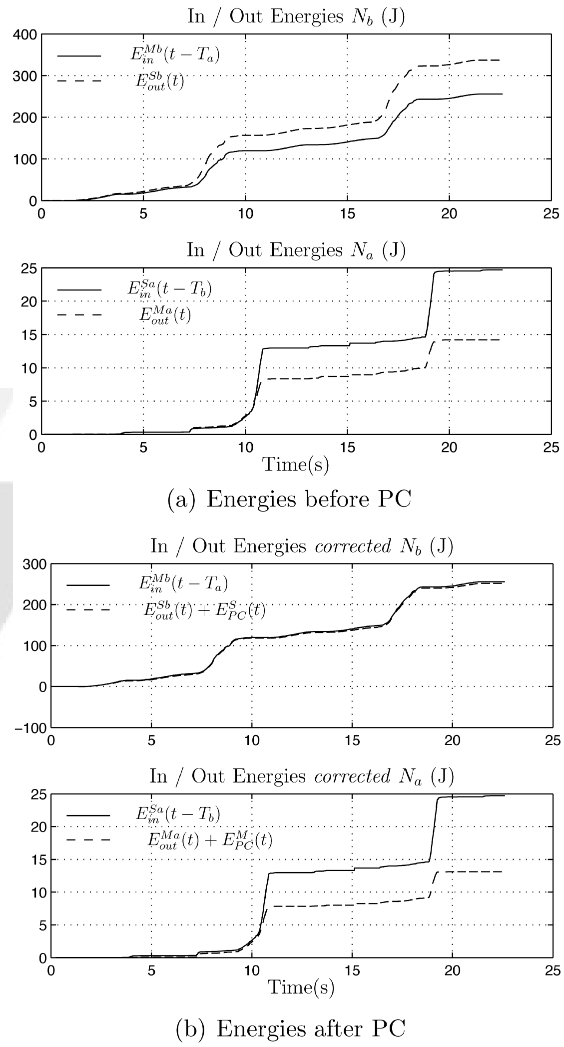

Figure 18. *Experimental data. 240 ms round trip delay. Contact.*

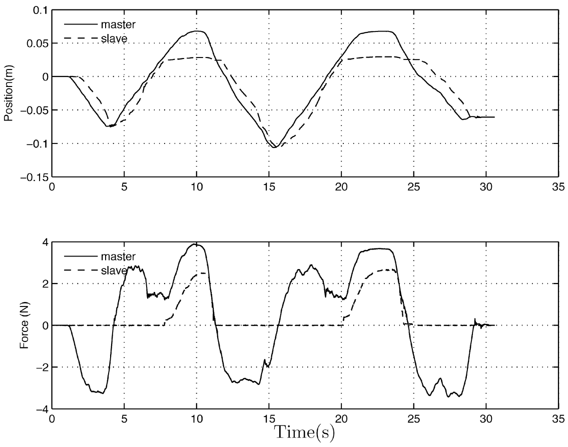

Figure 19. *Experimental data. 500 ms round trip delay. Contact.*

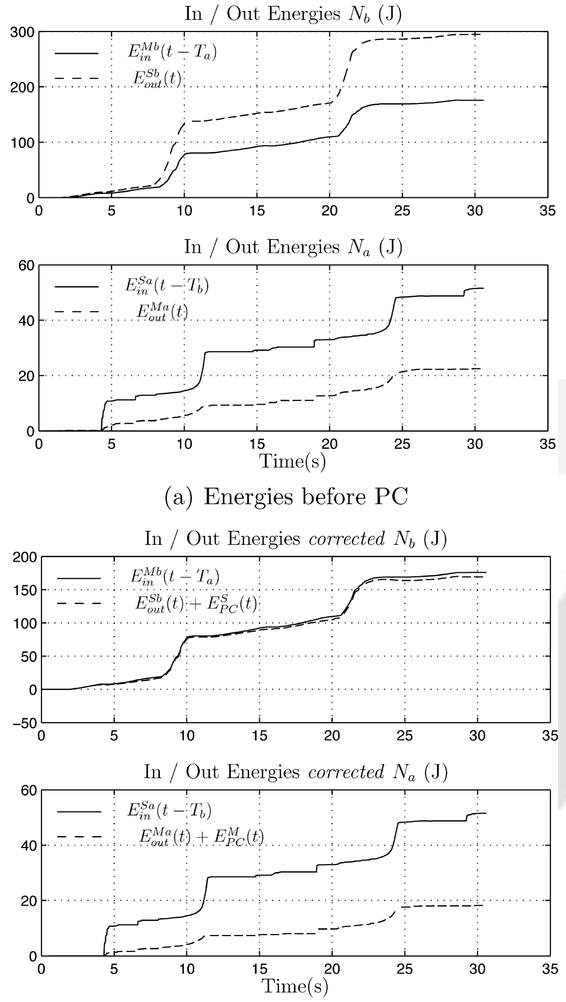

(a) Energies before PC

(b) Energies after PC

Figure 20. *Experimental data. 500 ms round trip delay. Contact.*

the two port network N_z can be represented by means of a pair of undelayed dependent current sources and 2 two port TDPNs, which convey the power generated by those current sources. These two networks, N_a and N_b, are responsible for channel activity and a cause of system instability. This new representation allows straightforward application of time domain passivity controller over the two TDPNs, N_a and N_b. The cascade connection of N_a and the BPC, and the cascade connection of N_b and the FPC, create passive networks for any amount of arbitrary constant or variable time delay. Apart from the analytical formulation, passivity of the system was sustained with a set of simulations and experiments that corroborate the feasibility of the method. This work can be regarded as a design methodology, which opens doors to other complex teleoperation architectures such as force-force, force-position, or the general four channel architecture (Lawrence, 1993).

Acknowledgments

This work was supported in part by the German Research Foundation (DFG) within the Collaborative Research Centre SFB 453 on High-Fidelity Telepresence and Teleaction.

References

Anderson, R. J., & Spong, M. W. (1989). Bilateral control of teleoperators with time delay. *IEEE Transactions on Automatic Control*, *34*(5), 494–501.

Artigas, J., Preusche, C., & Hirzinger, G. (2007). Time domain passivity for delayed haptic telepresence with energy reference. In *IEEE/RSJ International Conference on Intelligent Robots and Systems.* AQ2

Artigas, J., Preusche, C., Hirzinger, G., Borghesan, G., & Melchiorri, C. (2008). Bilateral energy transfer in delayed teleoperation on the time domain. In *Proceedings of the IEEE ICRA '08.* AQ3

Artigas, J., Preusche, C., Hirzinger, G., Borghesan, G., & Melchiorri, C. (2009). Bilateral energy transfer for high fidelity haptic telemanipulation. In *IEEE World Haptics 2009.* AQ4

Hannaford, B., & Ryu, J.-H. (2001). Time domain passivity control of haptic interfaces. In *Proceedings of the IEEE ICRA '01*, 1863–1869.

Hannaford, B., Ryu, J.-H., & Kim, Y. S. (2004). Sampled- and continuous-time passivity and stability of virtual environments. *IEEE Transactions on Robotics*, *20*(4), 772–776.

AQ5 Lawrence, D. A. (1993). Stability and transparency in bilateral teleoperation. *IEEE Transactions on Robotics and Automation*, *9*(5).

Lee, D., & Spong, M. W. (2006). Passive bilateral teleoperation with constant time-delay. *IEEE Transactions on Robotics and Automation*, *22*(2), 269–281.

Niemeyer, G. (1996). *Using wave variables in time delayed force reflecting teleoperation*. Ph.D. thesis, Massachussetts Institute of Technology, Cambridge, Massachusetts.

Ryu, J.-H., Hannaford, B., Preusche, C., & Hirzinger, G. (2003). Time domain passivity control with reference energy behavior. In *Proceedings of the 2003 IEEE/RSJ International Conference on Intelligent Robots and Systems.* AQ6

Ryu, J.-H., & Preusche, C. (2007). Stable bilateral control of teleoperators under time-varying communication delay: Time domain passivity approach. In *IEEE International Conference on Robotics and Automation*. AQ7

Secchi, C., Stramigioli, S., & Fantuzzi, C. (2007). *Control of interactive robotic interfaces: A post-Hamiltonian approach.* Vol. 29 of *Springer Tracks in Advanced Robotics.* Berlin: Springer Verlag. AQ8

Yokokohji, Y., & Yoshikawa, T. (1994). Bilateral control of master-slave manipulators for ideal kinesthetic coupling: Formulation and experiment. *IEEE Transactions on Robotics and Automation*, *10*(5), 605–620.

Author Queries

AQ1: Please confirm which is corresponding author.
AQ2: Please provide page numbers.
AQ3: Please provide page numbers.
AQ4: Please provide page numbers.
AQ5: Please provide page numbers.
AQ6: Please provide page numbers.
AQ7: Please provide page numbers.
AQ8: please check, “Tracks” or “Tracts”?